Supporting Information

Anti-inflammatory and antioxidant of skin based on supramolecular hyaluronic acid-ectoin

Beibei Lu[a,b,c,d,e], Siran Zhao[f], Jichuan Zhang[g], Jingbo Zhan[g], Jianglin Zhang[a,b,c,*], Zhe Liu[h,*], and Jiaheng Zhang[d,e,*]

[a]Department of Dermatology, Shenzhen People's Hospital (The Second Clinical Medical College, Jinan University; The First Affiliated Hospital, Southern University of Science and Technology), Shenzhen 518020, Guangdong, China.

[b]Candidate Branch of National Clinical Research Center for Skin Diseases, Shenzhen 518020, Guangdong, China.

[c]Department of Shenzhen People's Hospital Geriatrics Center, Shenzhen 518020, Guangdong, China.

[d]Sauvage Laboratory for Smart Materials, Harbin Institute of Technology (Shenzhen), Shenzhen 518055, P. R. China.

[e]Research Centre of Printed Flexible Electronics, School of Materials Science and Engineering, Harbin Institute of Technology (Shenzhen), Shenzhen 518055, P. R. China.

[f]Division of Chemistry and Analytical Science, National Institute of Metrology, Beijing, 100029, China.

[g]Shenzhen Shinehigh Innovation Technology Co., Ltd. Shenzhen 518055, P. R. China.

[h]Bloomage Biotech Co., Ltd. Jinan, Shandong 250104, China.

E-mail: zhang.jianglin@szhospital.com (Jianglin Zhang),
Liuzhe@bloomagebiotech.com (Zhe Liu),
zhangjiaheng@hit.edu.cn (Jiaheng Zhang).

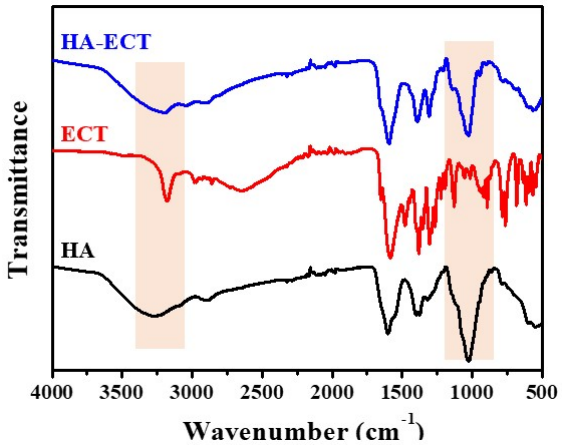

Figure S1. FTIR spectra of HA, ECT, and supramolecular HA-ECT.

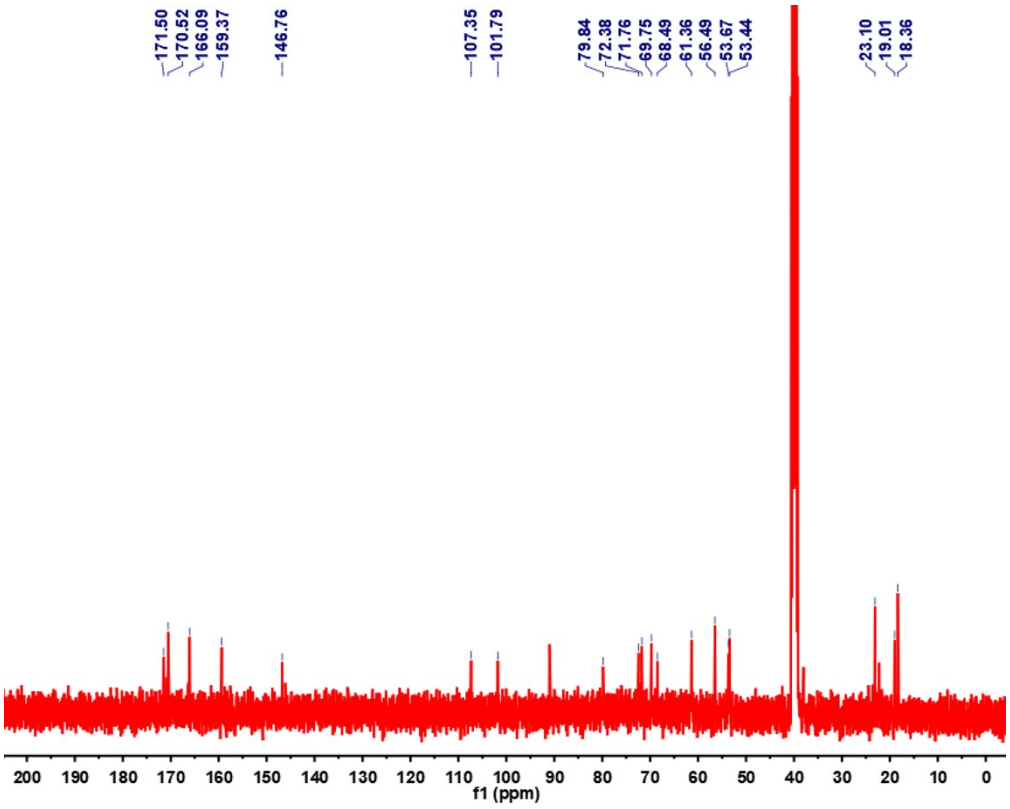

Figure S2. ^{13}C NMR spectrum of supramolecular HA-ECT.

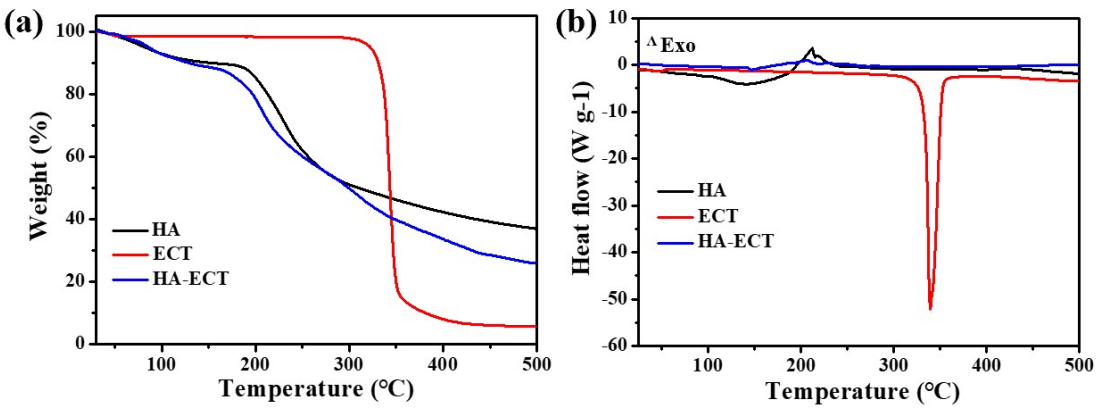

Figure S3. (a) TGA and (b) DSC images of HA, ECT, and HA-ECT.

The key resonance peak assignments of ^{1}H NMR in the DMSO-d_6 solvent system are shown in Table S1 (using the experimental group spectrum as an example), as shown in Figure S4. The experimental group samples generated an additional signal at 9.02 ppm, which was not a broad single peak characteristic of carboxyl groups but closer to the double peak of NH in HA, and still existed after water peak suppression (Figure S4). Therefore, based on its chemical shift, it is inferred that it belongs to the NH of HA, and from this, it was inferred that there are intramolecular or intermolecular hydrogen bonding interactions related to the NH of HA in the experimental group [1, 2].

Figures S5a-d show that the ^{1}H NMR spectra of two groups of samples were first collected in a DMSO-d_6: H_2O: D_2O=10:1:1 solvent system. The attribution of key resonance peaks is shown in Table S2 (using the experimental group spectrum as an example), and the spectral results are shown in Figure S5. In the new solvent system, the chemical shift of NH in ECT changed significantly, from 3.22 ppm to 9.38 ppm. The main difference between the experimental group and the mixed control group in ^{1}H NMR was also reflected in the NH of ECT. In the experimental group, NH=in ECT showed a broad single peak; In the mixed control group and ECT control group, the peak of the hydrogen spectrum was a sharper single peak. The change in peak shape reveals changes in intra - or inter-molecular interactions.

Based on ^{1}H NMR, two-dimensional NOESY spectra were further collected from the experimental group and the mixed control group. As shown in Figure S5e-f, the difference between the experimental group and the mixed control group reappears on

the cross peak generated by NH in HA. In the two spectra, from top to bottom, the NH of HA generates 5 types of cross peaks. The first type of cross peak was the correlation signal between NH of two types of HA and CH_2 of ECT or CH_3 of HA, the second type of cross peak was the correlation signal between NH of two types of HA and CH_3 of ECT, the third type of cross peak was the correlation signal between NH in HA and CH_2 in ECT, the fourth type of cross peak was the correlation signal between NH of HA and CH of HA's sugar skeleton, the fifth cross peak was the correlation signal between NH of HA and CH of ECT [1-4]. It can be observed that the relevant signals in the experimental group are generated between the NH of HA and the proton of ECT, while the relevant signals in the control group are generated between the HN of HA and the proton in HA. Based on the above information, a new intermolecular interaction has been formed between HA and ECT in the experimental group, and hydrogen bonds were formed between the NH of HA and the N or O atoms of ECT.

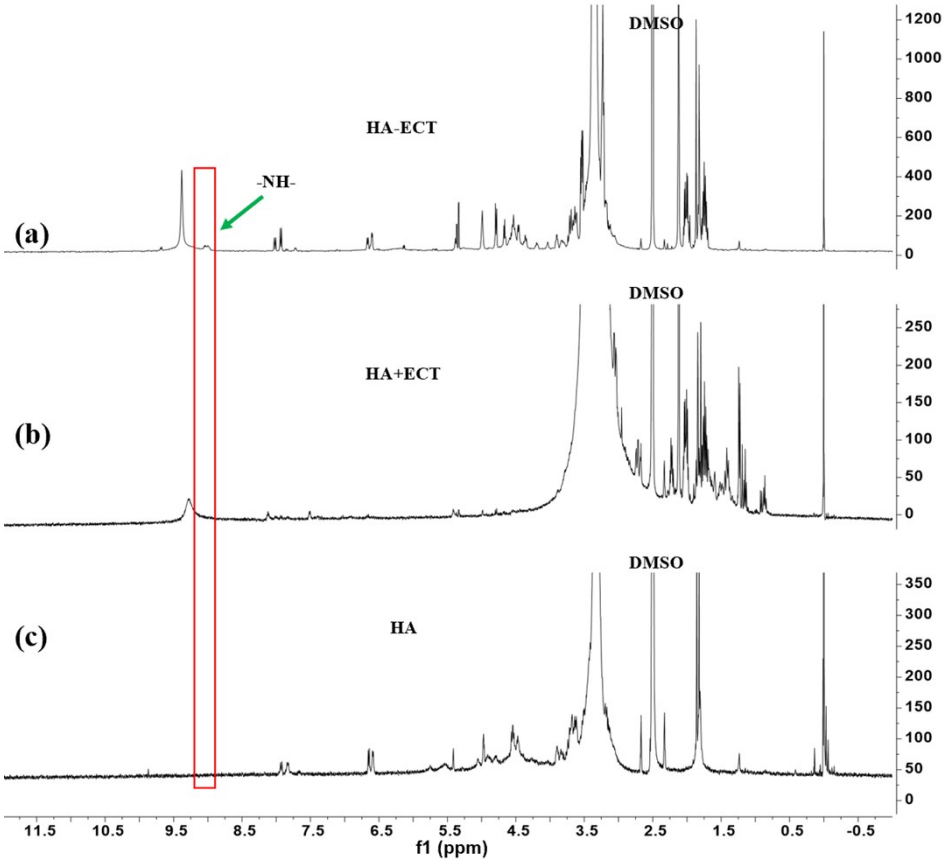

Figure S4. ^{1}H NMR spectrum of (a) supramolecular HA-ECT, (b) physical mixing HA+ECT, and (c) sodium hyaluronate in *DMSO-d_6* solvent system.

Table S1. The attribution positions of key resonance peaks in the ^{1}H NMR spectrum of the *DMSO-d_6* solvent system

Position		δ_H	Position		δ_H
ECT	CH_2-1	1.68-1.79 ppm, m	HA	CH_3	1.79-1.89 ppm, m
	CH_2-2	1.96-2.06 ppm, m		OH	6.56-6.70 ppm, m
	CH_3	2.12 ppm, s		NH	7.92 ppm, d, J = 7.7 Hz & 8.00 ppm, d, J = 7.7 Hz & 8.94-9.10 ppm, m
	NH	3.23 ppm, t, J = 5.0 Hz		CH	3.26-4.50 ppm, m
	CH	3.53 ppm, dd, J = 4.8 Hz, 7.5 Hz			
	COOH	9.38 ppm, bs			

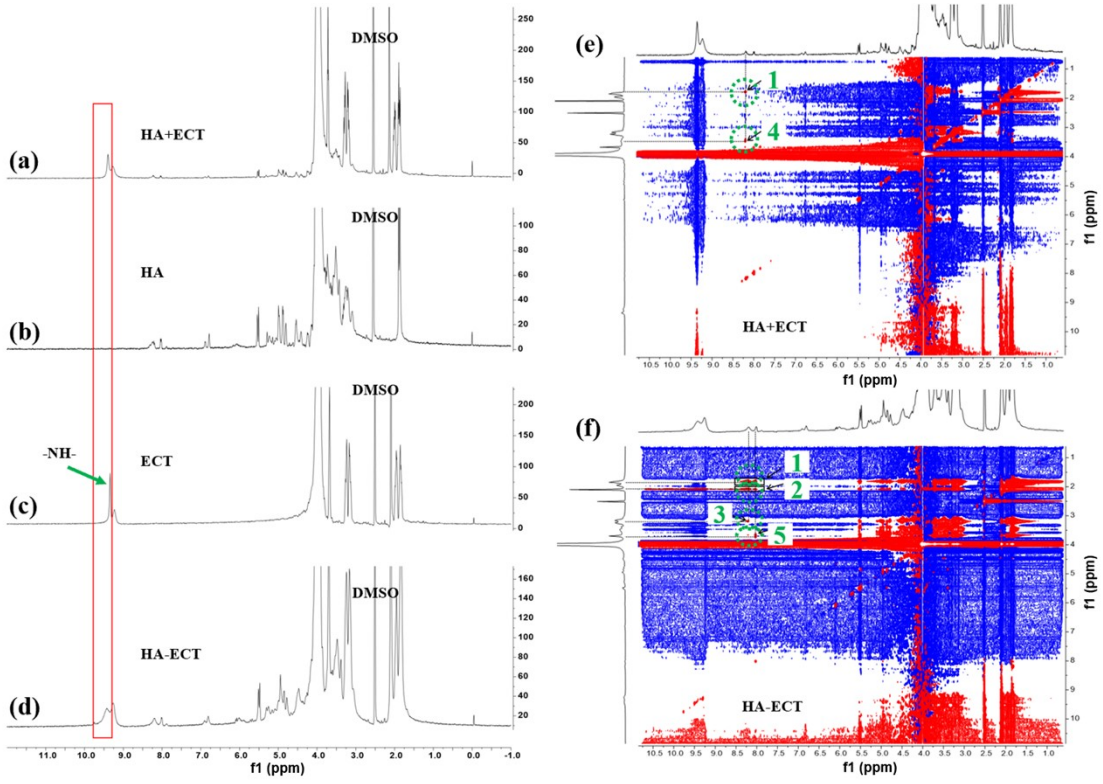

Figure S5. ^{1}H NMR spectra of (a) supramolecular HA-ECT, (b) HA, (c) ECT, and (d) physical mixing HA+ECT in *DMSO-d_6*: H_2O: D_2O=10:1:1 solvent system. NOESY spectra of (e) physical mixing HA+ECT and (f) supramolecular HA-ECT in *DMSO-d_6*: H_2O: D_2O=10:1:1 solvent system.

Table S2. The attribution positions of key resonance peaks in the ^{1}H NMR spectrum

of *DMSO-d*$_6$: H_2O: D_2O=10:1:1 solvent system

Position		δ_H	Position		δ_H
ECT	CH_2-1	1.79-2.07 ppm, m	HA	CH_3	1.81-1.93 ppm, m
	CH_2-2	3.10-3.37 ppm, m		OH	6.77-7.04 ppm, m
	CH_3	2.14 ppm, s		NH	8.00-8.52 ppm, m
	NH	9.46 ppm, s		CH	2.98-4.59 ppm, m
	CH	3.74 ppm, s			
	COOH	9.30 ppm, bs			

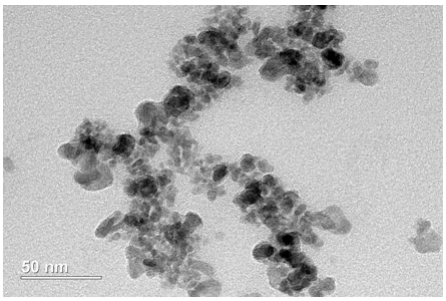

Figure S6. TEM image of physical mixture HA+ECT.

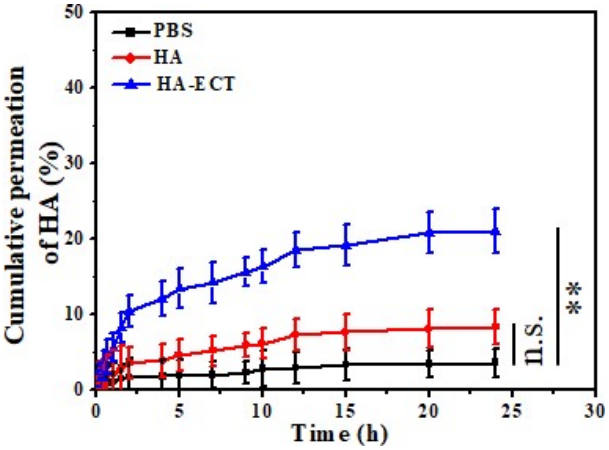

Figure S7. The cumulative amount of HA and HA-ECT percutaneous penetration. (n=6; *$p < 0.05$, **$p < 0.01$, ***$p < 0.001$, and n.s. represents no significant difference).

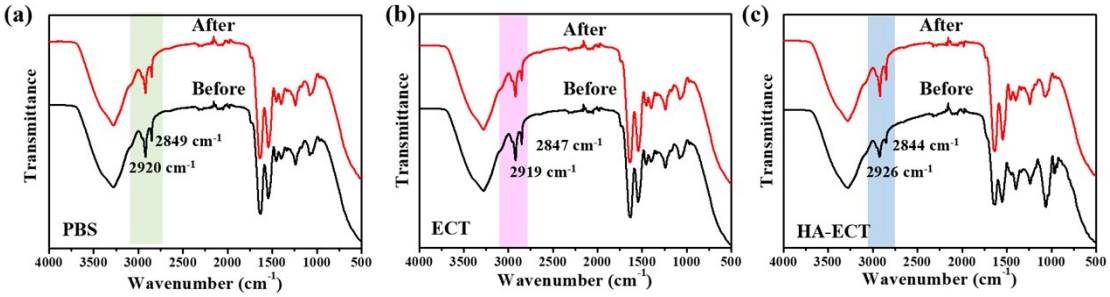

Figure S8. FTIR spectra of the skin before and after percutaneous penetration of (a) PBS, (b) ECT, and (c) supramolecular HA-ECT.

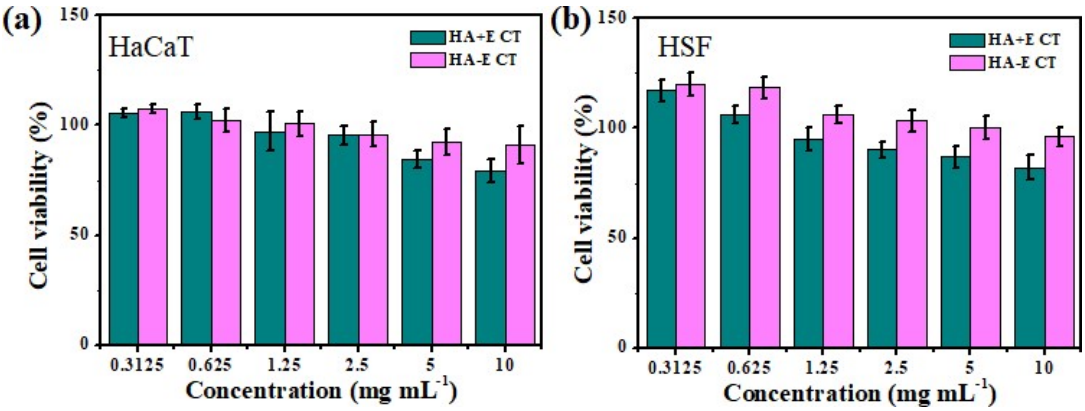

Figure S9. Cell viability of supramolecular HA-ECT and physical mixture HA+ECT to (a) HaCaT and (b) HSF cells at different concentrations.

Table S3. Experimental results of supramolecular HA-ECT patch test

Group	Number of subjects	Observation time	Number of people with different skin reactions in patch test [a]				
			0	1	2	3	4
Control	30	0.5	30	0	0	0	0
		24	30	0	0	0	0
		48	30	0	0	0	0
ECT	30	0.5	30	0	0	0	0
		24	30	0	0	0	0

		48	30	0	0	0	0
HA-ECT	30	0.5	30	0	0	0	0
		24	30	0	0	0	0
		48	30	0	0	0	0

[a]: 0 represents a negative reaction, 1 represents an able reaction, only weak erythema, 2 represents a weak positive reaction, erythema reaction, 3 represents a strong positive reaction, herpes reaction, 4 represents an extremely strong positive reaction, fusion herpes reaction.

Reference

[1] G. Nestor, C. Sandström. NMR study of hydroxy and amide protons in hyaluronan polymers. Carbohydr. Polym., 2017, 157, 920-928.

[2] P. Rampratap, A. Lasorsa, B. Perrone, P. C. A. Wel, M. T. C. Walvoort. Production of isotopically enriched high molecular weight hyaluronic acid and characterization by solid-state NMR. Carbohydr. Polym., 2023, 316, 121063-121071.

[3] M. Mende, M. Nieger, S. Bräse. Chemical synthesis of modified hyaluronic acid disaccharides. Chem. Eur. J., 2017, 7, 12283-12296.

[4] V. Malytskyi, J. Moreau, M. Callewaert, C. Henoumont, C. Cadiou, C. Feuillie, S. Laurent, M. Molinari, F. Chuburu. Synthesis and characterization of conjugated hyaluronic acids. Application to stability studies of chitosan-hyaluronic acid nanogels based on fluorescence resonance energy transfer. Gels, 2022, 8, 182-200.